

Preliminary Concepts for FWD Testing and Evaluation of Rigid Airfield Pavements

PAUL T. FOXWORTHY and MICHAEL I. DARTER

ABSTRACT

Results are presented of a study on the effects of temperature on repeatability of falling weight deflectometer (FWD) measurements, the behavior of rigid pavement joints, and the backcalculation of E and k in order to form the basis for application of finite element techniques to the classical Westergaard theory of rigid pavement evaluation. Three U.S. Air Force installations were chosen for an in-depth study of pavement response to FWD loads under a variety of environmental and geological conditions. Repeatability of FWD load and deflection measurements at constant temperatures as well as changing temperatures is reported. Effects of temperature on joint load transfer efficiency are analyzed, and predictive models are presented that account for seasonal temperature fluctuations in load-carrying capacity analyses of rigid pavements. A computer program to backcalculate elastic and subgrade reaction moduli from FWD deflection data has been developed, and repeatability of these moduli is established for different climatic conditions. The study has indicated the following: (a) the FWD is remarkably consistent in repeated load and deflection measurements at any slab position for constant temperatures; (b) center slab load and deflection measurements are also consistent under varying temperatures; (c) joint load transfer efficiency is highly temperature dependent but can be accurately modeled for a given joint type; and (d) E and k can be accurately determined from FWD measurements through an iterative computer scheme, and the results are consistent over a wide range of temperatures.

The current destructive test methodologies for obtaining critical airfield evaluation data and conducting the analyses are costly and time-consuming, but, most important, severely affect the operation of the airfield. In many cases the structural evaluation is neglected because airfield management cannot tolerate the schedule interruption that would occur with extensive downtime of the pavements. Fortunately, in recent years great strides have been made in the development of equipment that can rapidly and nondestructively collect data on which an evaluation of load-carrying capacity and future life can be made. Of particular importance in the evaluation of rigid airfield pavements was the development of impulse loading devices, such as the falling weight deflectometer (FWD), which reasonably approximate actual moving aircraft wheel loads (1). Simultaneously, researchers have been developing analytical models that could describe the response of a pavement system to specific loading conditions.

Presented in this paper are the results of several preliminary investigations that are essential in forming a solid foundation for the nondestructive testing and evaluation (NDT & E) of rigid airfield pavements. When coupled with other research done by the authors (see paper elsewhere in this Record), a complete system--including field testing, analyses, and prediction of future performance of each feature--is developed. Elsewhere, Foxworthy provides a comprehensive description of the entire study (2). Implementation of the system will permit rapid completion of field testing with little or no interruption of installation operations, and analysis of

field data and presentation of results are possible within hours.

TESTING EQUIPMENT AND PAVEMENT CHARACTERIZATION MODEL

An extensive investigation of available nondestructive equipment and engineering models led to the selection of the FWD and the ILLI-SLAB finite element program for this research. Each represents the latest advancements in the state of the art, but more important, they were selected because of the confidence the authors and other research and field engineers have in their ability to simulate actual loading conditions on airfield pavements (1,3).

The testing system is trailer mounted, towed a standard automobile, and weighs between 1,323 and 1,875 lb, depending on the weight of the falling mass used. By varying the drop heights and mass levels, impulse forces ranging between 1,500 and 24,000 lb can be achieved. Deflections are measured using up to seven velocity transducers mounted on a bar, which is lowered automatically with the loading plate. A typical configuration is shown in Figure 1. The entire operation can be controlled by one person from the front seat of the tow vehicle; typically 45 sec is required to complete an entire test sequence.

ILLI-SLAB was developed at the University of Illinois in the late 1970s for structural analysis of jointed, one- or two-layer concrete pavements with load transfer systems at the joints (4). The ILLI-SLAB model is based on the classical theory of a medium-thick plate on a Winkler foundation, and can evaluate the structural response of a concrete pavement system with joints, cracks, or both. Recent efforts by Ioannides et al. to revise and expand ILLI-SLAB have produced a versatile, easy-to-use tool with

P.T. Foxworthy, Civil Engineering Research Division, U.S. Air Force Weapons Laboratory, Kirtland AFB, N. Mex. 87111. M.I. Darter, University of Illinois, Urbana, Ill. 61801.

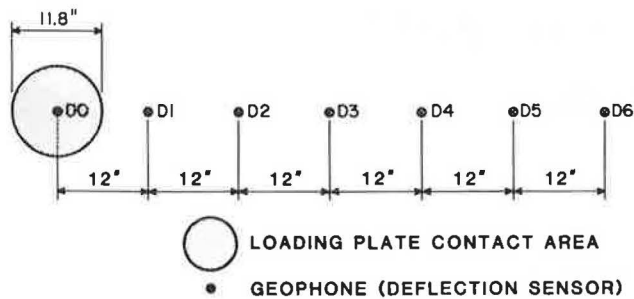


FIGURE 1 Typical location of the loading plate and deflection sensors of the FWD.

improved accuracy (5). Guidelines for proper mesh construction have been provided, and a global coordinate system is currently in place for easy use in analysis. The work by Ioannides has been instrumental in the development of the procedures used throughout this study.

FIELD RESEARCH PROGRAM

The engineer performing NDT & E of an airfield pavement system is faced with what must appear to be an overwhelming task of planning and executing the data collection program. The tremendous number of tests that are possible in a relatively short time period with the FWD permits great flexibility in evaluating many features and distress patterns. However, this flexibility also leads to a certain amount of perplexity in trying to plan the most efficient manner in which to collect and organize such a vast quantity of data. Adding to this confusion are the inevitable variabilities associated with the testing of non-homogeneous, anisotropic paving materials subjected to wide ranges in climatic conditions. A major objective of this research was to provide specific guidelines to the engineer for conducting the field testing program in light of these inherent variations; to this end, the field research program was designed.

With the introduction of NDT & E in the early 1960s, engineers began to experience significant variation in field test measurements over relatively short time periods. Such variations existed with destructive testing methods, but were largely ignored because of the expense involved in performing repeated testing. To date, little has been formally written on this problem, particularly in regard to rigid airfield pavements, either because equipment manufacturers were reluctant to publicize such information or because testing firms did not have the impetus to explore the problem.

This research effort has attempted to quantify this problem for several aspects of the rigid pavement evaluation process, including the following: (a) the repeatability of FWD deflection and load measurements at the center, edge, and corner of a slab over any given minute, hour, day, month, or season; (b) the effect of pavement, air temperature, or both on FWD deflection and load measurements, backcalculated slab and subgrade moduli, and load transfer efficiencies at joints; (c) the variation in portland cement concrete (PCC) elastic modulus, subgrade modulus, and load transfer efficiency from slab to slab within the same feature; (d) the effect of load magnitude on backcalculated moduli and load transfer efficiency; (e) the influence of type of joint construction on the relationship between load transfer efficiency and temperature; and (f) the consistency of load transfer efficiency along the joint.

FWD Measurement Repeatability

The first major concern addressed during the field research program was the repeatability of the FWD load and deflection measurements. If the validity of these measurements could be established, then confidence could be expressed in the equipment and a firm foundation could be laid for the analysis. To investigate this aspect of the data collection process, a testing program was conducted at Sheppard Air Force Base in Wichita Falls, Texas, to measure loads and deflections for several combinations of load, temperature, and thickness. This installation was selected because of its variety of pavement thicknesses and accessibility to key pavement features.

Testing for repeatability began by devising a test pattern for the FWD consisting of five points on each slab, three load levels, and four complete repetitions. This pattern was repeated for three slabs in each feature and for three features of different thicknesses. The entire test sequence for one slab took approximately 45 min to complete, thus minimizing the effects of air-pavement temperature change on the measurements. Each of the four series of drops at each point on the slab could have been performed consecutively, but by moving the FWD and then returning to approximately the same spot, it was believed that a more realistic measure of repeatability could be achieved.

Table 1 shows the repeatability of the FWD load/deflection ratio at constant temperature for Sheppard Feature T04A, Slab 1, at the corner position. An examination of the data in Table 1, typical of the results at slab joints and corners, reveals that appreciable improvement in the coefficient of variation of the load measurement can be expected as the load level increases. Load measurements typically average about 4 percent variation in the 7,000-lb range whereas deflections average about 5 percent. As loads increase to 15,000 lb, the variation in load measurement drops to about 2 percent whereas that of deflections remains about the same. Finally, 23,000-lb loads display about a 1 percent variation, whereas their corresponding deflections remain at about 5 percent. Results at the center slab positions were nearly identical for load measurements, but load/deflection ratios were even more consistent.

When raw deflection data are examined, good consistency is observed between the first and second drops (made within 30 sec of each other) and the third and fourth drops (also made within 30 sec of each other but nearly 30 min after the first two drops); however, the second pair of drops produced slightly lower deflections and loads, a definite trend that is attributable to increased temperatures in the rubber buffers of the FWD. Differences in the drops can also be partially accounted for by slight inaccuracies in repositioning the FWD and by rounding of the deflection values to the nearest one-tenth mil. However, overall the FWD exhibits remarkable consistency in measuring transient loads and small deflections on such nonuniform materials.

Results of repeatability measurements at constant air-pavement temperatures indicate that excellent consistency exists in FWD measurements for all points on the slab, but particularly at the center slab positions. Thus, the influence of the equipment on the variability of the end product, the backcalculated moduli and load transfer efficiency, is minimal. The contribution of time, temperature, and, to some extent, seasonal changes to the variation in FWD load and deflection measurements at center slab within hourly and daily periods was also examined. Moisture is presumed to play a modest role in the variations observed, but it is difficult to account for it apart from temperature over short time peri-

TABLE 1 Repeatability of FWD Load/Deflection Ratio at Constant Temperature

| Load ^a Range | Test No. | Load (lbf) | Sensor Load/Deflection Ratios | | | | | | |
|----------------------------|-------------|---------------|-------------------------------|------|------|-----------------|------|------|------|
| | | | D0 | D1 | D2 | D3 (lbf/mil) | D4 | D5 | D6 |
| Low | 1 | 7568 | 2225 | 4451 | 4370 | 5405 | 6306 | 6880 | 8408 |
| | 2 | 7360 | 2230 | 4906 | 4906 | 5661 | 6690 | 6690 | 8177 |
| | 3 | 6880 | 2372 | 4047 | 4586 | 5292 | 6254 | 6254 | 7644 |
| | 4 | 7088 | 2362 | 4430 | 4725 | 5452 | 5906 | 7088 | 7875 |
| | Average | 7224 | 2297 | 4458 | 4646 | 5452 | 6289 | 6728 | 8026 |
| Coef. of Var. | .04 | .04 | .08 | .05 | .03 | .05 | .05 | .04 | |
| Medium | 1 | 15536 | 1804 | 4510 | 4947 | 5477 | 6390 | 6970 | 8071 |
| | 2 | 15540 | 1828 | 4570 | 5012 | 5550 | 6475 | 7083 | 8178 |
| | 3 | 14912 | 1962 | 4030 | 4518 | 4970 | 5735 | 6778 | 7456 |
| | 4 | 14936 | 1890 | 4036 | 4392 | 4978 | 5744 | 6493 | 7468 |
| | Average | 15206 | 1871 | 4286 | 4717 | 5243 | 6086 | 6826 | 7793 |
| Coef. of Var. | .02 | .04 | .07 | .07 | .06 | .07 | .05 | .05 | |
| High | 1 | 22801 | 1727 | 4470 | 5066 | 5700 | 6514 | 7355 | 8444 |
| | 2 | 22817 | 1702 | 4563 | 5070 | 5565 | 6338 | 7130 | 8450 |
| | 3 | 22196 | 1834 | 4035 | 4624 | 5161 | 5841 | 6341 | 7653 |
| | 4 | 22483 | 1827 | 4087 | 4683 | 5228 | 5764 | 6612 | 7752 |
| | Average | 22574 | 1772 | 4288 | 4860 | 5413 | 6114 | 6859 | 8074 |
| Coef. of Var. | .01 | .04 | .06 | .05 | .05 | .06 | .07 | .05 | |

^aLoad ranges are as follows: low, 6,000 to 9,000 lbf; medium, 14,000 to 16,000 lbf; and high, 22,000 to 25,000 lbf.

ods. Therefore, only time and temperature differences are used in the comparisons. Seasonal variations in FWD measurements are also presumed to exist as a logical extension of daily variations, but this effect is most easily examined by using backcalculated moduli.

Load and deflection measurements were taken at four points on each slab, under several air temperature conditions but within the same 3-day period. Table 2 gives examples of the influence of air temperature fluctuations on FWD measurements made at center slab positions only (data are for Sheppard Feature T04A, Slab 1, at the center slab position). Joints and corners, as will be observed later, are significantly affected by air temperature changes, and therefore would not provide a meaningful comparison with the constant temperature case.

The trends displayed in this table closely parallel the findings for the constant temperature cases presented earlier. The coefficients of variation for load and particularly deflection measurements are noticeably better at the higher load levels. The modest 2 percent coefficient of variation in load/deflection ratios for high load levels over a 20-degree range in air temperature indicates that excellent consistency is available in FWD results at the center slab position. The 3 percent improvement in load/deflection ratio consistency over joint and corner positions that was measured under nearly constant temperature conditions demonstrates the strong dependency of joint and corner measurements on temperature.

The data in Table 3 present an interesting phenomenon that occurs as temperatures decrease. As air temperatures approach freezing, the FWD loads measured by the load cell increase significantly, but without a proportionate increase in the deflections. Loads that typically showed less than 2 percent variation in warm temperatures displayed 8 to 9 percent variation in cold temperatures, while deflections remained relatively unaffected.

It appears that for center slab conditions only, the moderate temperature fluctuations (15 to 20°F) experienced throughout the course of a normal test day do not add to the existing, constant temperature variation found in the equipment and pavement materials unless testing is done below 40 degrees. At these lower temperatures, the rubber buffers of the FWD apparently stiffen and impart a more sharply spiked impulse load to the pavement, creating higher load measurements. This same effect can also appear during early morning testing at air temperatures above 60 degrees. If the FWD has been stored overnight in cool conditions and the rubber buffers have not been allowed to warm up before testing, greater impulse loads will be imparted. The 8:00 a.m. reading on March 15 in Table 3 is a good example of this (data are for Sheppard Feature T04A, Slab 1, at the center slab position). However, these higher loads do not increase deflections appreciably. The results of this phenomenon on backcalculated moduli will be examined in more detail later in this paper.

JOINT LOAD TRANSFER

Joints have long been recognized as the major focal point for pavement distress in jointed concrete pavements, and yet are largely ignored in most of today's evaluation schemes. The load transfer efficiency of a joint, defined as the ratio of the deflection of the unloaded slab to the loaded slab, has a significant effect on the stresses that are developed at the bottom of the slab, and, therefore, on the performance of the slab under load. It quickly became evident during the field testing program that the high degree of repeatability of center slab load and deflection measurements did not exist at the joints as temperatures changed. Both the magnitude of the deflections and the load transfer efficiencies were affected.

TABLE 2 Repeatability of FWD Load/Deflection Ratio Under Varying Temperatures

| Load Range | Temp. Cond. No. | Load (lbf) | Sensor Load/Deflection Ratios | | | | | | |
|---------------|-----------------|------------|-------------------------------|------|------|------|-------|-------|-------|
| | | | D0 | D1 | D2 | D3 | D4 | D5 | D6 |
| Low | 1 | 8395 | 7631 | 8395 | 8395 | 9327 | 10493 | 11992 | 13991 |
| | 2 | 8300 | 7545 | 8300 | 8300 | 9222 | 9222 | 10375 | 13833 |
| | 3 | 8125 | 7386 | 8125 | 9027 | 9027 | 10156 | 10156 | 11607 |
| | 4 | 7998 | 7998 | 7998 | 8886 | 8886 | 9997 | 11425 | 11425 |
| | Average | 8205 | 7640 | 8204 | 8652 | 9115 | 9967 | 10987 | 12714 |
| Coef. of Var. | .02 | .03 | .02 | .04 | .02 | .05 | .08 | .11 | |
| Medium | 1 | 15534 | 6472 | 7397 | 7767 | 8175 | 9137 | 9708 | 11095 |
| | 2 | 15582 | 6492 | 7082 | 7420 | 7791 | 8656 | 9165 | 10368 |
| | 3 | 15852 | 6892 | 7205 | 7926 | 8343 | 8806 | 9324 | 11322 |
| | 4 | 15964 | 6940 | 7601 | 7982 | 8402 | 8868 | 9977 | 11402 |
| | Average | 15733 | 6699 | 7321 | 7773 | 8177 | 8866 | 9543 | 11051 |
| Coef. of Var. | .01 | .04 | .03 | .03 | .03 | .02 | .04 | .04 | |
| High | 1 | 23389 | 6496 | 7796 | 8065 | 8353 | 9355 | 10631 | 11694 |
| | 2 | 23484 | 6907 | 7575 | 7828 | 8387 | 9393 | 9785 | 11742 |
| | 3 | 23357 | 7077 | 7785 | 7785 | 8650 | 9342 | 10616 | 11678 |
| | 4 | 23071 | 6991 | 7690 | 7955 | 8544 | 9228 | 10486 | 11535 |
| | Average | 23325 | 6867 | 7711 | 7908 | 8483 | 9329 | 10379 | 11662 |
| Coef. of Var. | .01 | .04 | .01 | .02 | .02 | .01 | .04 | .01 | |

Note: Temperature Condition No. 1 existed on July 10 at 1:55 p.m. at an air temperature of 101°F. Temperature Condition No. 2 existed on July 11 at 8:45 a.m. at an air temperature of 89°F. Temperature Condition No. 3 existed on July 11 at 9:20 a.m. at an air temperature of 91°F. Temperature Condition No. 4 existed on July 12 at 10:00 a.m. at an air temperature of 82°F.

TABLE 3 Repeatability of FWD Load and Deflection Measurements Under Varying Temperatures

| Load Range | Temp. Cond. No. | Load (lbf) | Sensor Positions | | | | | | |
|---------------|-----------------|------------|------------------|------|------|------|------|------|------|
| | | | D0 | D1 | D2 | D3 | D4 | D5 | D6 |
| Low | 1 | 7304 | 1.1 | 1.0 | 0.9 | 0.9 | 0.7 | 0.7 | 0.6 |
| | 2 | 8376 | 1.1 | 1.0 | 1.0 | 0.9 | 0.9 | 0.7 | 0.7 |
| | 3 | 8848 | 1.2 | 1.0 | 1.0 | 1.0 | 0.9 | 0.8 | 0.7 |
| | 4 | 9632 | 1.1 | 1.0 | 1.0 | 1.0 | 0.8 | 0.8 | 0.7 |
| | Average | 8540 | 1.13 | 1.00 | 0.98 | 0.95 | 0.83 | 0.75 | 0.68 |
| Coef. of Var. | .11 | .04 | <.005 | .05 | .06 | .12 | .08 | .07 | |
| Medium | 1 | 15432 | 2.4 | 2.1 | 2.0 | 1.8 | 1.7 | 1.5 | 1.4 |
| | 2 | 16504 | 2.4 | 2.1 | 2.1 | 1.9 | 1.8 | 1.6 | 1.5 |
| | 3 | 17720 | 2.5 | 2.3 | 2.1 | 2.0 | 1.9 | 1.7 | 1.5 |
| | 4 | 18824 | 2.5 | 2.2 | 2.2 | 2.0 | 1.8 | 1.7 | 1.4 |
| | Average | 17120 | 2.45 | 2.18 | 2.10 | 1.93 | 1.75 | 1.63 | 1.45 |
| Coef. of Var. | .09 | .02 | .04 | .04 | .05 | .03 | .06 | .04 | |
| High | 1 | 23532 | 3.6 | 3.2 | 3.0 | 2.8 | 2.5 | 2.3 | 2.0 |
| | 2 | 24295 | 3.6 | 3.2 | 3.1 | 2.8 | 2.6 | 2.4 | 2.1 |
| | 3 | 25965 | 3.8 | 3.2 | 3.1 | 2.9 | 2.7 | 2.4 | 2.2 |
| | 4 | 28318 | 3.7 | 3.3 | 3.2 | 2.9 | 2.7 | 2.4 | 2.0 |
| | Average | 25527 | 3.68 | 3.23 | 3.10 | 2.85 | 2.63 | 2.38 | 2.08 |
| Coef. of Var. | .08 | .03 | .02 | .03 | .02 | .04 | .02 | .05 | |

Note: Temperature Condition No. 1 existed on March 13 at 12:30 p.m. at an air temperature of 61°F. Temperature Condition No. 2 existed on March 15 at 8:00 a.m. at an air temperature of 65°F. Temperature Condition No. 3 existed on March 17 at 4:15 a.m. at an air temperature of 45°F. Temperature Condition No. 4 existed on March 19 at 8:20 a.m. at an air temperature of 36°F.

Load Transfer Efficiency

The importance of load transfer at joints on the overall performance of rigid airfield pavements is intuitively obvious but not well documented. A perfectly efficient system for transferring load from one side of the joint to the other can reduce the free edge stress by 50 percent (6,7). Many different systems have been developed and tested for establishing and maintaining high degrees of load transfer across joints during the life of the pavement. The objective of these systems is simple: to minimize the tensile stresses and deflections in the concrete that result when loads are applied at the edge of the slab. Keeping concrete edge stresses at a minimum dramatically reduces fatigue damage and greatly increases pavement life, while reducing deflections minimizes the potential for pumping.

In the evaluation of remaining pavement structural life, the level of stress developed under an aircraft gear at the slab joint must be determined. Unfortunately, it is impractical to quickly or economically measure actual stresses developed at joints. However, it is possible to determine how well the load transfer mechanism is performing by measuring the relative deflection on both sides of the joint. This relative deflection is a direct indication of the load transfer efficiency of the joint. Normally, a correction

is applied to the deflection measured by the D1 sensor (see Figure 1) to account for slab curvature due to bending, but the finite element mesh has been designed to automatically make this adjustment. By coupling the load transfer efficiency with a good analytical model of joint behavior, such as ILLI-SLAB, the edge stresses under actual loads can be calculated.

Effect of Load Magnitude on Load Transfer Efficiency

To investigate the possibility that the load transfer efficiency at joints is dependent on the magnitude of the loads used to create the relative deflections, the data presented in Table 4 were extracted from the constant temperature repeatability study discussed earlier. These data represent three slab thicknesses, two joint types, loads from 6,500 to 24,000 lb, and load transfer efficiencies between 30 and 100 percent.

The results given in Table 4 support the conclusion that load transfer efficiency is independent of the load magnitude, at least within the load range of the FWD (this may not be true for light load devices that generate loads less than 5,000 lb). With the exception of Slab 1 in Feature T04A, load trans-

TABLE 4 Relationship Between Magnitude of Load and Load Transfer Efficiency as Measured at Undoweled Transverse Contraction Joints and Keyed Longitudinal Construction Joints

| Feature | Slab No. | Undoweled Transverse Contraction | | | | Keyed Longitudinal Construction | | | |
|---------|----------|----------------------------------|-----------|-----------|---------|---------------------------------|-----------|-----------|---------|
| | | Load (lbf) | D0 (mils) | D1 (mils) | LTE (%) | Load (lbf) | D0 (mils) | D1 (mils) | LTE (%) |
| T04A | 1 | 7456 | 1.6 | 1.2 | 75 | 6936 | 1.8 | 1.2 | 67 |
| | | 15400 | 3.9 | 2.6 | 67 | 15032 | 4.3 | 2.4 | 56 |
| | | 23055 | 6.1 | 3.7 | 61 | 23103 | 6.7 | 3.4 | 51 |
| | 2 | 6840 | 1.1 | 0.9 | 82 | 6968 | 1.3 | 1.2 | 92 |
| | | 14648 | 2.6 | 2.2 | 85 | 14640 | 3.0 | 2.7 | 90 |
| | | 22514 | 3.9 | 3.4 | 87 | 22673 | 4.4 | 4.1 | 93 |
| | 3 | 6752 | 1.2 | 1.2 | 100 | 6688 | 1.5 | 1.3 | 87 |
| | | 14656 | 2.8 | 2.7 | 96 | 14808 | 3.4 | 3.1 | 91 |
| | | 23150 | 4.2 | 4.1 | 98 | 22848 | 5.2 | 4.6 | 88 |
| A03B | 1 | 7496 | 1.8 | 1.7 | 94 | 7216 | 2.3 | 0.9 | 39 |
| | | 16296 | 4.0 | 3.8 | 95 | 15496 | 4.9 | 2.2 | 45 |
| | | 23914 | 6.0 | 5.7 | 95 | 23421 | 7.3 | 3.4 | 47 |
| | 2 | 7528 | 5.0 | 2.7 | 54 | 7400 | 4.5 | 4.0 | 89 |
| | | 15368 | 11.4 | 5.2 | 46 | 15512 | 9.6 | 8.3 | 86 |
| | | 23246 | 17.6 | 7.3 | 41 | 23373 | 14.4 | 12.2 | 85 |
| | 3 | 6872 | 3.1 | 1.0 | 32 | 6936 | 2.8 | 1.0 | 36 |
| | | 14992 | 7.4 | 2.3 | 31 | 15064 | 6.4 | 1.9 | 30 |
| | | 23071 | 11.3 | 3.6 | 32 | 23150 | 9.5 | 2.8 | 29 |
| A05B | 1 | 6888 | 1.6 | 1.5 | 94 | 6896 | 2.1 | 1.8 | 86 |
| | | 14936 | 3.6 | 3.3 | 92 | 14944 | 4.8 | 4.3 | 90 |
| | | 22801 | 5.4 | 5.0 | 93 | 22976 | 7.2 | 6.5 | 90 |
| | 2 | 6680 | 1.9 | 1.9 | 100 | 6792 | 2.2 | 1.9 | 86 |
| | | 14840 | 4.5 | 4.3 | 96 | 14824 | 5.1 | 4.4 | 86 |
| | | 22928 | 6.6 | 6.4 | 97 | 22769 | 7.6 | 6.6 | 87 |
| | 4 | 7696 | 2.1 | 2.0 | 95 | 7240 | 2.3 | 2.1 | 91 |
| | | 15584 | 4.5 | 4.2 | 93 | 15280 | 4.8 | 4.4 | 92 |
| | | 23532 | 6.6 | 6.2 | 94 | 23007 | 7.2 | 6.5 | 90 |

fer efficiencies are remarkably consistent, particularly in view of the inherent variation in the equipment and materials highlighted earlier. With this result, the extrapolation of load transfer efficiencies under actual aircraft loadings can be made confidently.

Variation of Load Transfer Efficiency Along the Joint

Two additional aspects of joint load transfer that the engineer must be concerned with during field testing are (a) the direction in which the relative deflections are measured, and (b) the location of the measurement along the joint. It has been demonstrated that, for example, on highway pavements load transfer efficiency measured with the loading plate on the approach slab is much different from when measured from the leave slab (8). In addition, the highly channelized nature of highway traffic causes variation in load transfer efficiency along the joint. To investigate these concerns for airfield pavements, 21 positions on 3 slabs for 3 separate pavements were tested at low and high temperatures. Typical results of this investigation are shown in Figure 2 (data are for Feature T04A, Slab 1). Two sets of measurements are included to dramatize the effect that temperature has on load transfer efficiency.

Several general trends can be observed from these results. First, there appears to be little difference in load transfer efficiency at transverse joints when measured from the approach or leave slabs. This conclusion is not surprising for the airfield situation

in which traffic is usually bi-directional along taxilines and centerlines. However, for longitudinal joints this is not the case. Several slabs show marked increases in load transfer efficiency when measured from the leave slab, indicating that loading history can influence joint behavior. Again, this result is not surprising when it is considered that aircraft gears ride consistently along the same side of the longitudinal joint, regardless of the direction of travel. Therefore, the engineer must determine where the majority of the gears track and adjust his test pattern accordingly.

Load transfer efficiencies are consistent, for the most part, along the joint. This permits some latitude in trying to position the FWD somewhere near the aircraft gearpath on the slab. However, in several instances the efficiencies drop off as the corner of the slab is approached. This tendency could result from loss of subbase support at the corner, and thus the effect of shear in the base or subgrade, or it could be due to the absence of dowel bars near the corners in each of the adjacent slabs. In any event, the normal test pattern is intended to identify potential problem areas near corners. Finally, the effect of increased temperature on load transfer efficiency is unmistakable; significant increases in joint performance accompany higher temperatures. This effect will be examined in more detail.

Effect of Temperature on Load Transfer Efficiency

One of the most disturbing aspects of NDT & E of any pavement system is the variability of results due to temperature. In flexible pavement systems, this effect is most pronounced on the stiffness of the asphaltic concrete materials. In rigid pavements, temperature changes influence load transfer efficiency more than any other characteristic of the system. Although temperature has been known to affect load transfer for some time, no attempts have been made to accurately quantify this phenomenon. One of the major objectives of this research effort was to describe the behavior of different joint types under changing temperature conditions. From this background, it was expected that a technique could be developed to account for the temperature effect in predicting the remaining life of rigid pavements. This temperature effect is undoubtedly composed of both curling effects and expansion and contraction effects, but only the combined effect is considered important in joint load transfer efficiency.

The repetitive nature of the FWD testing at Sheppard Air Force Base, coupled with the extremes in temperature that are routinely experienced in field testing, provided the basis on which to quantify load transfer changes with temperature. Load transfer efficiencies were measured at 20 dummy groove transverse joints and 20 keyed longitudinal joints, encompassing a range of pavement thicknesses from 10 to 20 in. Dowelled joints were not available for testing and, therefore, are not included in this study. Pavement surface temperatures were recorded for each test by inserting a digital thermometer probe into a predrilled, 1-in. deep, 1/8-in. diameter, oil-filled hole in each slab. Air temperatures were also obtained from the base weather station for each hour with the view that either could be used for analysis. A minimum of 5, and generally 12, temperature levels were obtained for each joint.

Figures 3 and 4 are graphic displays of the distinct relationship between joint load transfer efficiency and air temperature over a wide spectrum (for Feature T04A). The highly significant aspect of this behavior lies in the characteristic shape of this

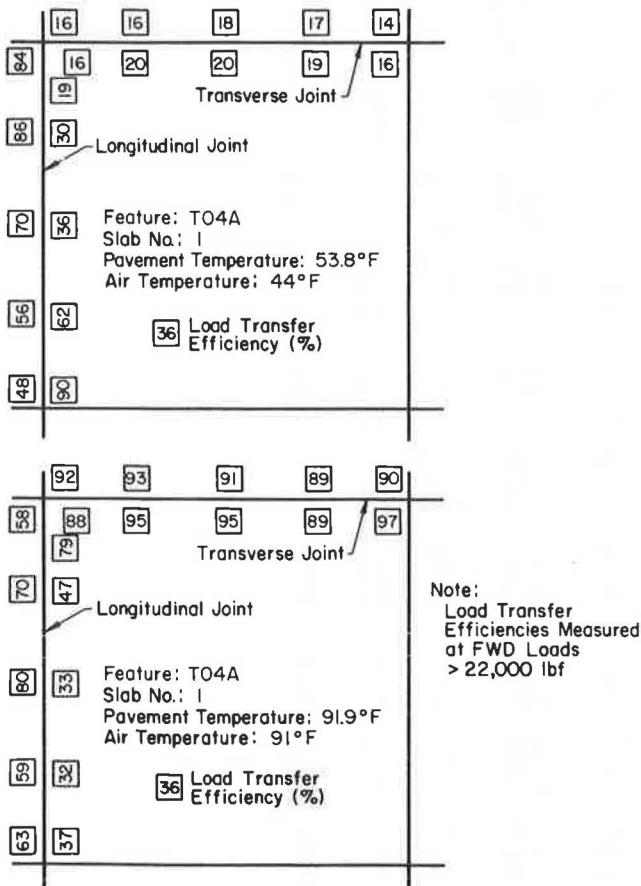


FIGURE 2 Joint load transfer efficiencies at various locations.

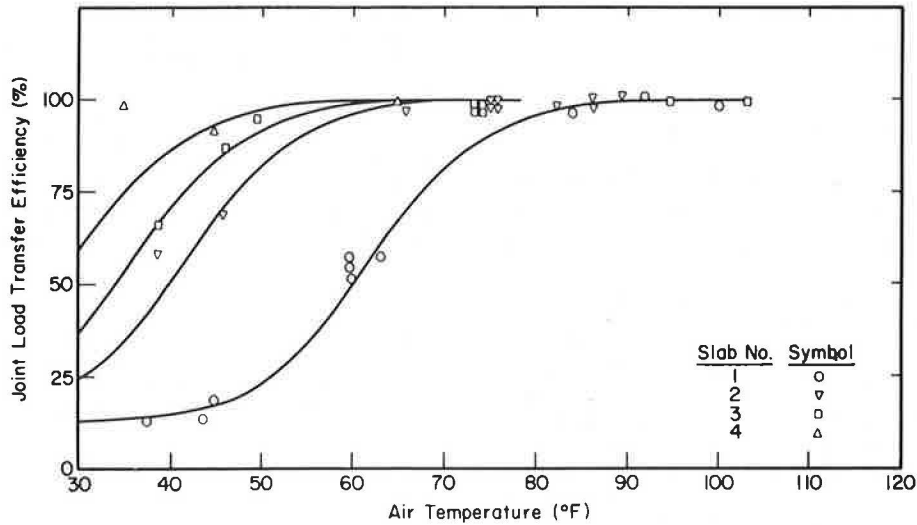


FIGURE 3 Relationship between air temperature and transverse joint load transfer efficiency.

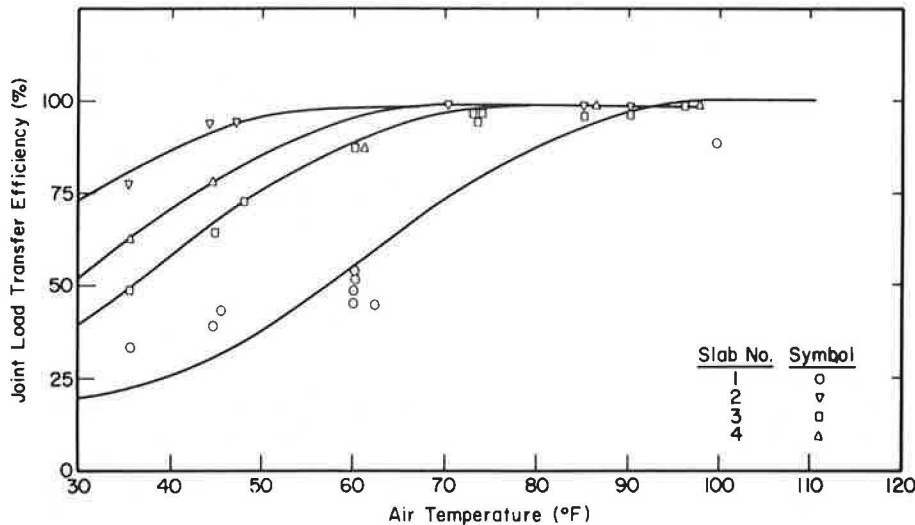


FIGURE 4 Relationship between air temperature and longitudinal joint load transfer efficiency.

relationship, an S-shaped curve. Each joint appears to take on the same shape and is nearly identical for both pavement temperature and air temperature. The variety of horizontally shifted positions for joints within the same feature is typical, and makes it difficult to select a joint that is representative of the entire feature.

Each joint tends toward a maximum load transfer efficiency of 100 percent as temperatures increase, and toward a minimum value of 20 to 25 percent as temperatures decrease. In many instances, the joint opening is so small that good load transfer exists throughout the temperature range, regardless of how much the slab contracts. In contrast, some joints have such poor load transfer at all temperatures in the normal range that they display a nearly flat response. However, this behavior does not mean that the characteristic shape of the load transfer efficiency-temperature curve cannot be described by an S-shaped curve. It merely means that the curve is shifted significantly, in either direction, from the norm.

The explanation for this consistent behavior is

complex and involves the interaction of aggregate particles along the face of the transverse crack, or the contact between the male and female portions of the longitudinal keyed joint. Presumably, as the joint opens up under falling temperatures, less concrete surface area is available for contact and deflection resistance. When the joint opens completely, a certain minimum amount of load transfer is still available through the shear strength of the base course or subgrade material. Thus, the upper bound of 100 percent and a somewhat variable lower bound of 20 to 25 percent are reasonable. Additional research might correlate the lower bound with the material type used directly beneath the PCC surface.

With upper and lower bounds established, the only characteristic of the curve remaining to be identified is the slope, or rate at which the load transfer efficiency approaches the bounds. Inspection of Figures 3 and 4 reveals that each curve of similar joint type has approximately the same slope, and that a distinctly steeper slope exists for transverse dummy groove joints than for the longitudinal keyed joints. It appears that the type of joint construc-

tion affects the rate at which load transfer diminishes with temperature, which is not a surprising result.

Prediction of Load Transfer Efficiency

The discovery that the load transfer efficiency-temperature relationship of a given joint type closely follows an S-shape curve with certain upper and lower bounds and diminishing rate makes it possible to establish the horizontal location of this curve for any joint, if the load transfer efficiency at some temperature is known. However, this is precisely what is determined in the field with the FWD. Therefore, it becomes possible to rely on only one measurement of load transfer efficiency for a joint to predict the efficiency that will occur for any temperature that joint might experience. Only in those instances in which measured load transfer efficiency is near the upper or lower bound are additional measurements recommended. This can mean tremendous savings in personnel and equipment costs in field data collection; retesting of the same joint at several temperatures to determine its behavior pattern is eliminated. In addition, knowing the load transfer efficiency for the entire temperature range permits a much more accurate determination of cumulative fatigue damage from aircraft operations over an entire year.

An S-shaped curve with a positive slope has the following general form:

$$LTE = A_1 + (A_2 - A_1)e^{-(SF/AT)^{A_3}} \quad (1)$$

where

- LTE = load transfer efficiency,
- A₁ = lower bound,
- A₂ = upper bound,
- SF = shift factor in kelvin,
- AT = air temperature in kelvin, and
- A₃ = slope at inflection point.

Note that the air temperature and shift factor must be converted to the absolute scale to avoid the

mathematical impossibilities that would occur when temperatures at or below zero on either the Fahrenheit or Centigrade scale are encountered. Figure 5 shows the generalized form of the S-shaped curve and its five fundamental parameters.

In Equation 1, the values of the constants A₁ and A₂ were determined by inspection of many data plots similar to those in Figures 3 and 4, whereas the value of A₃ must be determined for each type of joint construction. This was done using the Non-linear Computer Analysis of the Statistical Package for the Social Sciences (SPSS) (9). The value of A₃ was calculated for each of the 20 transverse joints and 20 longitudinal joints and averaged to obtain a single curve that describes the load transfer efficiency versus temperature relationship for that joint type. The following equations were developed for each joint type:

For transverse dummy groove joints:

$$LTE = 0.25 + 0.75e^{-(SF/AT)^{40.0}} \quad (2)$$

For longitudinal keyed joints:

$$LTE = 0.25 + 0.75e^{-(SF/AT)^{25.0}} \quad (3)$$

These two equations can now be used to predict the load transfer efficiency that will exist at a given joint for any temperature if the load transfer efficiency is known for only one temperature. In making this calculation, it is assumed that the load transfer efficiency measured in the field lies somewhere between 25 and 100 percent, exclusive. Otherwise, the shift factor cannot be determined uniquely for that joint.

BACKCALCULATION OF CONCRETE ELASTIC MODULUS AND MODULUS OF SUBGRADE REACTION

When any type of load is placed on a rigid pavement slab, the slab will deflect nearly vertically to form a basin. The deflected shape of that basin is a function of several variables, including the thickness of the slab, the stiffness of the slab (characterized by E), the stiffness of the underlying

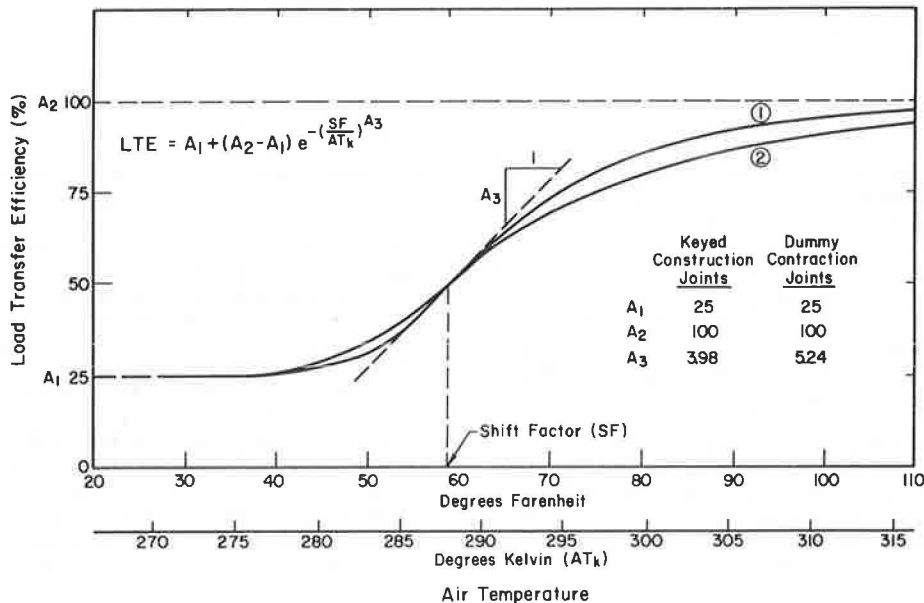


FIGURE 5 Generalized S-shaped curve and its fundamental parameters.

support systems (characterized by k), and the magnitude of the load. This interaction between E and k results in a characteristic deflection basin for a given magnitude and duration of load and thickness of concrete. If the approximate shape of the basin can be measured under loading conditions similar to an aircraft gear, and if two independent parameters describing the shape of the basin can be developed, then a unique value for both E and k can be backcalculated for a given load and slab configuration.

Hoffman and Thompson (10) found that it was possible to characterize a two-parameter model for flexible pavements by using the maximum deflection under the load (D_0) and a parameter they called the basin area. This area concept, shown in Figure 6, combines all the measured deflections in the basin into a single number to minimize the effect of an erroneous geophone reading. The area being determined

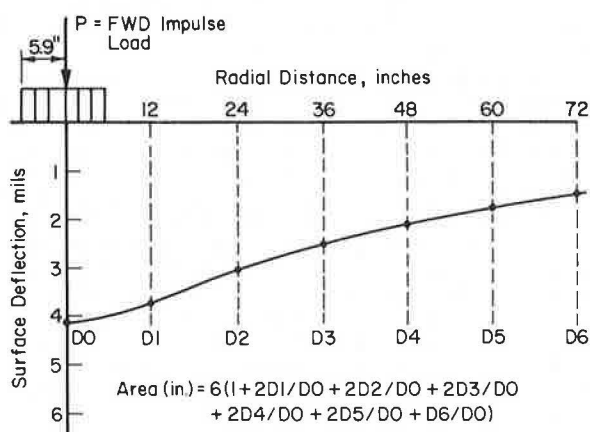


FIGURE 6 Deflection basin area concept.

is essentially one-half of the cross-sectional area of the deflection basin taken through the center of the load. To eliminate the effect of variable loads and to restrict the maximum and minimum values of the area, each deflection reading is normalized with respect to the maximum D_0 deflection. Thus, the basin area has the units of length and is a function of the number and location of the sensors. Using the FWD with seven sensors spaced 12-in. apart and the trapezoidal rule, the following equation is employed to calculate area for rigid pavements:

$$\begin{aligned} \text{Area (in.)} = & 6 \times (1 + 2 \times D_1/D_0 + 2 \times D_2/D_0 + 2 \\ & \times D_3/D_0 + 2 \times D_4/D_0 + 2 \times D_5/D_0 \\ & + D_6/D_0) \end{aligned} \quad (4)$$

By visualizing a perfectly stiff slab, that is, all deflections equal, the maximum area possible from Equation 4 is 72 in. Conversely, a practical minimum area of about 11 is obtained if Boussinesq techniques are employed (the slab is as stiff as the foundation).

The independence of the D_0 and area parameters is assured by the normalizing process. The same D_0 could produce an area of 72 in. just as easily as one of 11 in. With the deflection basin area and the maximum deflection D_0 , it is possible to solve for that unique combination of dynamic E and k that produces the same characteristic basin as measured with the FWD.

The determination of dynamic E and k from deflection basin measurements can be accomplished graphically for any given slab configuration, Poisson's ratio of the concrete, and magnitude of load. This

technique has proven successful in backcalculating dynamic E and k values that, when input back into the ILLI-SLAB model, very accurately reproduce FWD-measured deflections (7). However, its use has been limited primarily to thinner highway pavements on which only four sensors on the FWD are needed to describe the deflection basin accurately.

Several drawbacks to this graphic technique should be noted because they severely limit its application for large airfield evaluation programs. First, this technique requires hand plotting of the backcalculation grid, which can only be done after several ILLI-SLAB computer runs have been annually input. Second, a new grid must be developed for each pavement thickness and slab size encountered, which can mean up to 25 separate grid formulations for each airfield. Third, individual FWD deflections must be normalized to a standard load, usually 24,000 lb, to avoid a separate grid for each drop of the FWD. Finally, inaccuracies can easily be introduced through poor interpolation of dynamic E and k values within the grid. This source of error can be minimized somewhat, but only if more ILLI-SLAB runs are made to develop a finer grid.

Computer-Based Iterative Solution for Dynamic E and k

One of the major objectives of this research was to develop a complete, computer-based rigid pavement evaluation system that would relieve the engineer of hand manipulation of large amounts of data. Initially, efforts centered on the development of a large, computer-generated data base from which algorithms for estimating dynamic E and k , given the deflection basin characteristics and the geometry of the slab, could be formulated. Although showing some potential, these efforts failed to produce the accuracies that could be obtained from the graphic solutions.

Consequently, a simple iterative scheme was devised by using ILLI-SLAB as a computer subroutine that accurately backcalculates the unique dynamic E and k combination by matching measured and observed deflections. The program contains checks after each iteration and terminates when prescribed tolerances are satisfied. Up to five iterations may be required to close within these tolerances, but three or four iterations are typical. The greater sensitivity of both area and D_0 in the higher ranges of E and k will dictate how many iterations are ultimately required. A complete description of the technique involved in this computer solution for E and k can be found in a paper by Foxworthy (2).

Comparison of Measured and Predicted Deflection Basins

The validity of any analytical model is truly tested when predicted response is compared with measured response. To verify the accuracy of ILLI-SLAB and the backcalculated dynamic E and k moduli, each individual slab at Sheppard Air Force Base was used to compare measured and predicted deflections for FWD loads of more than 22,000 lb. Figure 7 graphically shows the results for one feature (Feature A06B). This figure shows the outstanding precision with which ILLI-SLAB models a pavement's response to load.

An analysis of the deflection data reveals trends similar to those established during the FWD repeatability study. As deflections decrease away from the loaded area, the percent error between measured and predicted deflection at each sensor tends to increase. This is reasonable if each sensor carries about the same built-in error (the sensors are ac-

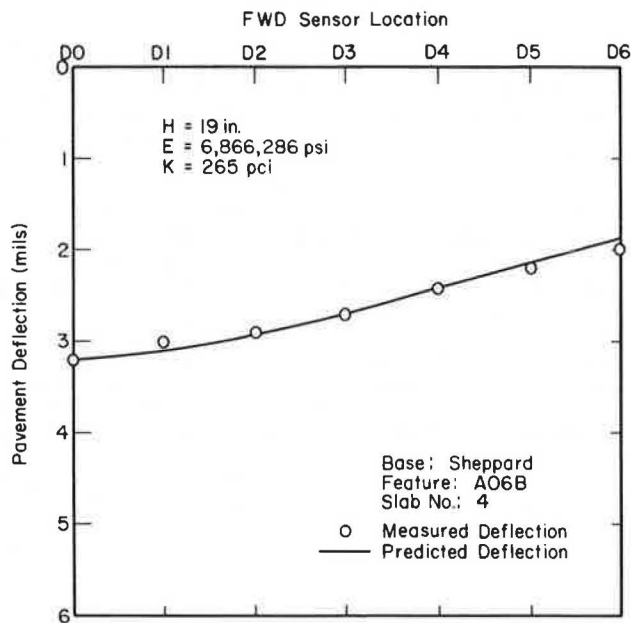


FIGURE 7 Comparison of measured and predicted FWD deflections.

curate to within 0.0005 in.). Typically, 1 to 2 percent error is observed for the D0 reading whereas 5 to 6 percent is common for the D6 value. However, in most cases this match between measured and predicted deflection basins is remarkable, particularly in light of the inherent variation in the sensors and paving materials, and the very small deflections involved.

Repeatability of Backcalculated Dynamic E and k Moduli

Table 5 gives the results of backcalculated dynamic moduli at constant temperature for two features at Sheppard Air Force Base. Each table entry for the given temperature (e.g., 78.6, 82.2, etc.) represents at least eight tests performed within 45 min of each other. Several important conclusions can be drawn from this table and the results of extensive analyses of variance.

First, at slab center, no apparent relationship exists between the magnitude of load and k, other than a decrease in the coefficient of variation of k as load increases for these features. This indicates that the dynamic k is not stress sensitive for the interior FWD loads used or the base and subgrade materials involved.

Second, although the coefficients of variation decrease with increased load, they remain somewhat higher for backcalculated k than those observed for FWD-measured loads and deflections.

Third, a pattern does exist with regard to dynamic E values and magnitude of load. Consistently higher, and often unrealistic, dynamic E values are backcalculated for low load levels, as evidence by Feature A05B in Table 5. The differences are much more pronounced between low and medium loads than between medium and high loads. The coefficients of variation for dynamic E values display much the same tendencies, with the higher loads showing significantly greater consistency. Again, higher load levels appear to give more realistic and reliable results, suggesting that the highest load levels attainable with the FWD should be used. Unrealistic values of E or k can be flagged by the computer for further study.

One of the most puzzling aspects of NDT & E is the effect of changing environmental conditions on

TABLE 5 Repeatability of Backcalculated Dynamic E and k Moduli at Constant Temperature at the Center Slab Position

| Feature | Slab No. | Pvmt Temp. (°F) | Load ^a Range | k | | E x 10 ⁶ | | No. of Tests |
|---------|----------|-----------------|-------------------------|---------------|---------------|---------------------|---------------|--------------|
| | | | | Average (pci) | Coef. of Var. | Average (psi) | Coef. of Var. | |
| T04A | 1 | 78.6 | Low | 294 | .19 | 4.2 | .33 | 8 |
| | | | Medium | 280 | .15 | 3.8 | .26 | 8 |
| | | | High | 286 | .11 | 3.6 | .18 | 8 |
| | 2 | 82.2 | Low | 434 | .09 | 2.9 | .13 | 8 |
| | | | Medium | 349 | .07 | 3.3 | .14 | 8 |
| | | | High | 358 | .07 | 3.2 | .12 | 8 |
| | 3 | 80.8 | Low | 206 | .14 | 5.5 | .15 | 8 |
| | | | Medium | 205 | .17 | 4.7 | .27 | 8 |
| | | | High | 215 | .12 | 4.6 | .22 | 8 |
| A05B | 1 | 68.4 | Low | 181 | .11 | 6.6 | .18 | 9 |
| | | | Medium | 178 | .16 | 6.0 | .11 | 9 |
| | | | High | 190 | .05 | 5.8 | .12 | 9 |
| | 2 | 74.5 | Low | 156 | .12 | 7.9 | .17 | 8 |
| | | | Medium | 158 | .04 | 6.9 | .04 | 8 |
| | | | High | 181 | .06 | 6.2 | .08 | 8 |
| | 4 | 89.1 | Low | 125 | .18 | 7.9 | .29 | 8 |
| | | | Medium | 141 | .07 | 6.0 | .13 | 8 |
| | | | High | 150 | .05 | 5.7 | .07 | 8 |

^aLoad ranges are as follows: low, 6,000 to 9,000 lbf; medium, 14,000 to 17,000 lbf; and high, 22,000 to 26,000 lbf.

the parameters that characterize the pavement system. Individual E- and k-value trends with pavement temperature indicate that all slabs within a feature display similar tendencies, but no overall predictable pattern is discernible. Dynamic k values tend to be slightly higher at colder temperatures, level off in mid-range, and then increase again slightly at higher temperatures. This kind of pattern would appear to be related more to moisture levels than temperature, but additional research into this aspect is needed to reach any meaningful conclusions. In any event, the fluctuation in k is not significant enough to affect the stresses generated to any great extent. Dynamic E values also exhibit a pattern similar to k values, tending to be moderately higher at colder temperatures and then leveling off. However, at higher temperatures the pattern is inconsistent.

Table 6 presents a summary of the results of backcalculated dynamic k and E values for eight slabs at pavement temperatures ranging from 36 to 101 °F. With at least five cases per slab, this table shows that the introduction of temperature as a variable has increased the coefficients of variation above the levels established by the constant temperature situation, particularly for dynamic E values at low load levels. At recommended high load levels, this increase in the coefficient of variation is modest, averaging about 4 percent. Dynamic k values remain relatively unaffected by temperature fluctuations,

with coefficients of variation similar to the constant temperature case. Figure 8 shows how the normal variation in E and k at constant temperatures is great enough to encompass the variation in E and k at different temperatures.

In conclusion, it appears that only temperature extremes substantially influence backcalculated dynamic E and k values. Temperature fluctuations between 40 and 90°F are relatively insignificant, producing little variation in addition to that which is already inherent in the equipment and pavement materials. The overwhelming temperature effect occurs at the joints, where load transfer plays an important role in the pavement response to load.

SUMMARY

The foundation for a complete system that will non-destructively test and evaluate rigid airfield pavements has been developed. The FWD has been shown to give consistent load and deflection measurements under a variety of temperature and slab location conditions. The effects of changing temperatures on joint load transfer efficiency have been described, and mathematical models have been formulated to incorporate these relationships into actual stress analyses. Finally, an iterative solution for E and k, based on FWD measurements, permits their consis-

TABLE 6 Repeatability of Backcalculated Dynamic E and k Moduli at Various Temperatures at the Center Slab Position

| Feature | Slab No. | Pvmt Temp. Range (°F) | Load ^a Range (lbf) | k | | E x 10 ⁶ | | No. of Cases |
|---------|----------|-----------------------|-------------------------------|---------------|---------------|---------------------|---------------|--------------|
| | | | | Average (pci) | Coef. of Var. | Average (psi) | Coef. of Var. | |
| T04A | 1 | 33.1 to 121.8 | Low | 275 | .19 | 5.9 | .31 | 8 |
| | | | Medium | 276 | .15 | 4.2 | .16 | 8 |
| | | | High | 316 | .13 | 3.6 | .19 | 8 |
| | 2 | 33.1 to 121.8 | Low | 422 | .13 | 4.7 | .26 | 8 |
| | | | Medium | 348 | .12 | 4.4 | .27 | 8 |
| | | | High | 396 | .10 | 3.8 | .27 | 8 |
| | 3 | 33.1 to 121.8 | Low | 268 | .29 | 5.8 | .38 | 8 |
| | | | Medium | 243 | .27 | 1.3 | .27 | 8 |
| | | | High | 261 | .25 | 4.6 | .26 | 8 |
| | 4 | 33.1 to 121.8 | Low | 448 | .24 | 2.9 | .53 | 5 |
| | | | Medium | 370 | .13 | 4.4 | .08 | 5 |
| | | | High | 391 | .12 | 4.2 | .12 | 5 |
| A05B | 1 | 34.2 to 119.3 | Low | 209 | .17 | 7.1 | .13 | 6 |
| | | | Medium | 189 | .16 | 7.2 | .13 | 6 |
| | | | High | 208 | .18 | 6.5 | .09 | 6 |
| | 2 | 34.2 to 119.3 | Low | 194 | .31 | 9.1 | .33 | 7 |
| | | | Medium | 176 | .16 | 7.7 | .21 | 7 |
| | | | High | 188 | .08 | 7.6 | .14 | 7 |
| | 3 | 34.2 to 119.3 | Low | 327 | .23 | 10.0 | .19 | 6 |
| | | | Medium | 287 | .12 | 9.3 | .24 | 6 |
| | | | High | 310 | .09 | 8.8 | .09 | 6 |
| | 4 | 34.2 to 119.3 | Low | 189 | .14 | 7.5 | .27 | 7 |
| | | | Medium | 173 | .10 | 6.8 | .15 | 7 |
| | | | High | 182 | .07 | 6.8 | .11 | 7 |

^aLoad ranges are as follows: low, 6,000 to 9,000 lbf; medium, 14,000 to 16,000 lbf; and high, 22,000 to 25,000 lbf.

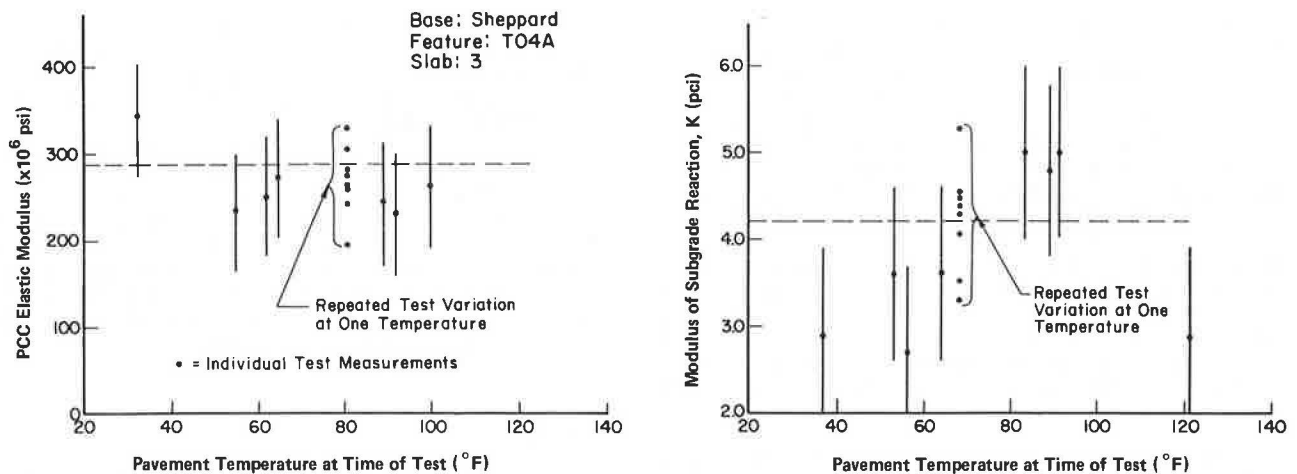


FIGURE 8 Typical variation in E and k at constant temperature applied to single observations of E and k at various temperatures.

tent determination under a wide range of temperatures.

ACKNOWLEDGMENTS

The authors wish to acknowledge the cooperation and financial support of the U.S. Air Force Engineering and Services Center and the University of Illinois, without which this research could not have been accomplished.

REFERENCES

1. R.E. Smith and R.L. Lytton. Synthesis Study of Nondestructive Testing Devices for Use in Overlay Thickness Design of Flexible Pavements. ERES Consultants, Champaign, Ill., Nov. 1983.
2. P.T. Foxworthy. Concepts for the Development of a Nondestructive Testing and Evaluation System for Rigid Airfield Pavements. Ph.D. dissertation. University of Illinois at Urbana-Champaign, Urbana, 1985.
3. A.M. Tabatabaie, E.J. Barenberg, and R.E. Smith. Longitudinal Joint Systems in Slip-Formed Rigid Pavements. Volume II--Analysis of Load Transfer Systems for Concrete Pavements. Report FAA-RD-79-4. Federal Aviation Administration, U.S. Department of Transportation, Nov. 1979.
4. A.M. Tabatabaie-Raissi. Structural Analysis of Concrete Pavement Joints. Ph.D. dissertation. University of Illinois, Urbana, 1977.
5. A.M. Ioannides, J. Donnelly, M.R. Thompson, and E.J. Barenberg. Analysis of Slabs-On-Grade for a Variety of Loading and Support Conditions. AFOSR-83-0143. U.S. Air Force Office of Scientific Research, Washington, D.C., Sept. 1984.
6. M.I. Darter. Concrete Pavement Evaluation. Proc., 7th Annual Airport Engineering and Safety Seminar, Federal Aviation Administration, Hershey, Penn., March 1983.
7. Nondestructive Structural Evaluation of Airfield Pavements. ERES Consultants, Champaign, Ill., Dec. 1982.
8. J.A. Crovetto and M.I. Darter. Joint Repair Methods for Portland Cement Concrete Pavements, Appendix C, Void Detection Procedures. University of Illinois, Urbana, March 1985.
9. N.H. Nie et al. Statistical Package for the Social Sciences. McGraw-Hill, New York, 1975 (2nd edition).
10. M.S. Hoffman and M.R. Thompson. Mechanistic Interpretation of Nondestructive Pavement Testing Deflections. Project IHR-508, University of Illinois, Urbana, June 1981.

Publication of this paper sponsored by Committee on Monitoring, Evaluation and Data Storage.